UNIVERSITY OF CALIFORNIA SAN DIEGO

Wnt signalling through FZD receptors: The structure and function of FZD7

A Thesis submitted in partial satisfaction of the requirements
for the degree Master of Science

in

Biology

by

Neya Suresh Kumar

Committee in charge:

Professor Karl Willert, Chair
Professor David Traver, Co-Chair
Professor Heidi Cook-Andersen

2020

The Thesis of Neya Suresh Kumar is approved and it is acceptable in quality and form for publication on microfilm and electronically:

_____

_____

Co- Chair

_____

Chair

University of California San Diego

2020

TABLE OF CONTENTS

LIST OF FIGURES

ABSTRACT OF THE THESIS

Wnt signaling through FZD receptors: The structure and function of FZD7

by

Neya Suresh Kumar

Master of Science in Biology

University of California San Diego, 2020

Professor Karl Willert, Chair

Professor David Traver, Co-Chair

Wnt signalling plays a critical role in development, producing signals that regulate stem cell self-renewal and differentiation. Wnt signalling is initiated when a Wnt ligand binds to a Frizzled (FZD) receptor on the cell surface membrane. The mammalian genome encodes 19 Wnt and 10 Fzd genes, however, relatively little is known about specific interactions between individual Wnts and FZDs. Complicating studies to investigate Wnt-FZD

interactions is that Wnt ligands are highly hydrophobic, making them difficult to purify in a biologically active form. Here, we are investigating the utility of a novel Wnt agonist that simultaneously binds FZD7 and a co-receptor encoded by the LRP6 gene to activate downstream signalling. The Wnt mimetic is highly specific to FZD7, so I was able to identify a minimal epitope of 8 amino acids necessary for binding. I showed that engineering this tag onto other FZD receptors such as FZD2 and FZD9 was sufficient to force heterodimerization of these FZDs with LRP6 using the Wnt mimetic, and thus able to activate signal transduction. I also investigated the importance of different domains in FZD7 for β-catenin dependent signaling by generating several truncations and deletions in FZD7 and generating chimeric FZD receptors between FZD7 and FZD9. This revealed that transmembrane domains and c-terminal tail are critical for FZD7 function, while the cysteine rich domain of the FZD receptor dictates ability to bind with Wnt ligands but not signaling ability.

Introduction:

A fertilized oocyte goes from a single cell to form complex organisms through a coordinated execution of several cell signaling processes and divisions. A key pathway that regulates embryonic development is Wnt signaling (Stenman *et al.*,2008). Wnt signaling is sufficient to induce the primitive streak, a morphological feature of the early embryo where germ layer formation is first initiated in the vertebrate embryo (Martyn *et al.*,2018). Beyond that, Wnt signaling controls cell polarity, axis determination, and stem cell differentiation and renewal (Komiya and Habas, 2008). As this pathway is central to the early development of invertebrates and vertebrates, it is highly conserved across the animal kingdom (Miller, 2002; Croce and Mcclay, 2011). Dysregulation of the Wnt signaling pathway has been implicated in a wide variety of diseases from autoimmune diseases to several types of cancer (Zimmerman *et al.*,2012).

Downstream Wnt signaling can occur through the β-catenin (canonical) pathway or the β-catenin independent (non-canonical) pathway. Wnts are secreted molecules that bind to cell surface receptors to initiate signaling (Willert and Nusse, 2012). The canonical pathway is as follows. In the Wnt-off state, a destruction complex comprised of APC, Axin and GSK3 binds and phosphorylates free β-catenin in the cytoplasm. The phosphorylated β-catenin is then ubquitinated and degraded by the proteasome (Macdonald *et al.*, 2010), and Wnt target gene expression remains repressed due to DNA bound T-cell factor/lymphoid enhancer factor (TCF/LEF). β-catenin dependent (canonical) Wnt signaling requires the presence of both a Frizzled (FZD) and its coreceptor, Low Density Lipoprotein Receptor-related Protein (LRP) 5 or 6 (Tamai *et al.*, 2000). The FZD receptors are 7-pass transmembrane proteins on the cell surface membrane with an extracellular cysteine rich domain (CRD) and an intracellular C-terminal tail. Wnt proteins bind directly to the CRD of the FZD (Dann *et al.*, 2001, Janda et al. 2012). When Wnt binds to the FZD receptor and its coreceptor LRP5/6, they

heterodimerize and recruit Dishevelled, a signaling molecule, to the complex. The recruitment of Dishevelled to the intracellular portion of the FZD receptor leads to the phosphorylation of LRP 5/6 and the disassembly of the destruction complex. Free of its destruction complex, β-catenin accumulates in the cytoplasm, allowing it to translocate into the nucleus and complex with TCF/LEF factors. This turns on Wnt target gene expression, which regulates a multitude of developmental processes. Humans express 19 different Wnt ligands and 10 different Frizzled (FZD) receptors. Relatively little is known about how individual Wnt/FZD pairings regulate downstream signaling (Macdonald *et al.*,2010).

Studying the Wnt signaling pathway is complicated because Wnt ligands are difficult to isolate in a biologically active form, and their binding to the FZD-LRP5/6 receptor complexes is thought to be highly promiscuous as a single Wnt ligand can bind and activate several FZD receptors simultaneously (Dijksterhuis *et al.*, 2015, Voloshanenko et al. 2017). Since the majority of Wnts are not available in a soluble form, their interactions with various FZD receptors have not been explored. Further complicating Wnt-FZD binding studies is the fact that Wnt proteins are lipid modified, rendering them highly hydrophobic and necessitating detergents to maintain their solubility (Willert et al., 2003); such detergents interfere with measurements of ligand-receptor interactions. Furthermore, detergents are not compatible with biological systems and, hence, application of purified Wnt proteins in vivo is often not possible. The lack of available soluble Wnt proteins makes it difficult to activate specific receptors to study their signaling pathway (Mulligan *et al.*, 2011). As a result, most studies on FZD receptors have been conducted through overexpression and knockdown approaches and observing a phenotypic change (Voloshanenko et al. 2017).

Individual FZD genes play many distinct roles in embryonic development and in adult tissue homeostasis. For example, FZD4 is implicated in the establishment and maintenance of the blood brain barrier and retinal vascularization (Wang *et al.*, 2016). FZD6 has been shown

to regulate hair follicle orientation in early development (Chang *et al.*,2016). However, FZD gene knockout or knockdown does not always yield a phenotypic change. This can be seen in the case of FZD8 and FZD10, as a loss of function of these receptors shows no phenotypic change despite these FZDs being widely expressed in tissues (Wang *et al.*,2016). In some cases, such as FZD7, loss of function produces mild effects, such as tail kinking, a phenotype consistent with the role of Wnt/FZD signaling in formation of the anterior-posterior axis (Yu *et al.,* 2012). Such lack of robust phenotypes is likely due to biological redundancy in the role of different FZD receptor or to potential compensation by other FZD receptors to make up for the loss of one receptor. Therefore, a limitation of studying biological function through knocking down gene expression is that it does not always result in a phenotypic change.

FZD7 is particularly interesting as it plays significant roles in two seemingly distant processes; embryogenesis and carcinogenesis (Nusse, 2005). One of the 10 FZD receptors, FZD7 has been well characterized in its role to maintain pluripotency of human embryonic stem cells (Fernandez *et al.*,2014). FZD7 has also been studied extensively for its role in cancer. For example, Pode-Shakked *et al.* demonstrated that FZD7 is a biomarker in Wilm's tumor, a rare kidney cancer, and went on to show that FZD7-positive cells are highly proliferative and maintained stem cell markers (2010). This suggests that FZD7 signaling in cancer activates stem-like properties, implicating FZD7 in several cancer types. Upregulation of FZD7 expression is seen in a variety of tumors, including gastric cancer, esophageal cancer and melanoma (Tanaka *et al.*, 1998; Kirikoshi *et al.*,2001; Sagara *et al.,* 1998). Ueno K *et al.,* showed that a knock down of FZD7 mRNA in colon cancer cells led to a lower expression of β-catenin target genes, showing that FZD7 most likely signals canonically in cancer (Ueno *et al.,* 2009). Furthermore, an antibody, called vantictumab, that binds the CRD of FZD7 was shown to inhibit canonical Wnt signaling, which resulted in the inhibition

human tumor xenograft growth (Gurney *et al.*,2012). This points to FZD7 playing a key role in cancer through β-catenin dependent signaling.

In Wnt/FZD signaling, the CRD of the FZD receptor facilitates binding to specific Wnt ligands (Dijksterhuis *et al.*,2015)(Figure 1). Following Wnt binding, the cytoplasmic scaffolding protein Dishevelled (DVL) is recruited to the signaling complex. However, it is not yet known if other proteins are involved in DVL recruitment of FZD. The highly conserved KTXXXW motif in the C-terminal tail immediately after the seventh transmembrane domain (TM) of FZD is essential for activating β-catenin dependent signaling (Umbhauer *et al.*,2000), potentially through binding of DVL (Bertalovitz *et al*, 2016). By understanding how FZD7 transduces signaling will aid in the development of therapies directly targeting these regions and potentially inhibiting the signal in the context of cancer.

The activation of FZD7 through Wnt ligands, with high affinity ligand-receptor binding, is a potential way to answer which intercellular components of a FZD receptor mediates signaling. This was done through testing mutated, truncated and chimeric FZD7 receptors for signaling activity using a Wnt3a ligand. Wnt3a, like most Wnts, is highly promiscuous and binds to several FZD receptors. Most cells express a variety of FZDs on their cell surface and signaling due to FZD7/Wnt3a interaction would be difficult to study. To work around this, these constructs were tested in a Wnt3a insensitive system where HEK293T cells had FZD 1, 2 and 7 knocked out (Voloshanenko *et al.*,2017). Using this system the authors were able to probe the ability of various FZDs, including FZD7, to transduce the Wnt3a signal. These experiments established that Wnt3a could signal efficiently through FZD1, 2, 4, 5, 7 and 10.

Another area of focus is understanding the biological role of FZD receptors through specific activation, as Wnt ligands lack binding specificity to FZD receptors. To circumvent this issue, the Willert lab has developed a novel bispecific binder composed of single chain

antibody variable fragments that mimics the action of Wnt, by binding specifically to FZD7 and its coreceptor LRP 5/6 (Gumber et al., manuscript in preparation). Just like native Wnt proteins, the Wnt mimetic causes FZD7 and LRP5/6 to heterodimerize, causing signaling down the β-catenin dependent (canonical) pathway (Gumber et al., manuscript in preparation). As the Wnt mimetic is composed of antibody subunits, it can be easily purified using the constant region of the immunoglobulin (Ig) heavy chain. Since this Wnt mimetic is not lipid modified like Wnt, it is soluble in biological environments without the need of detergents. Use of the Wnt mimetic provides an avenue for the specific and independent activation of FZD7. The lab has shown that the Wnt mimetic is able to specifically activate FZD7 and turn on Wnt target genes (Gumber et al., manuscript in preparation).

Here, I describe my experiments to further characterize the signaling functions of FZD7. To do so, I used both purified Wnt3a protein and the FZD7-specific Wnt mimetic, which, unlike Wnt3a, uniquely activates only FZD7. By mutating and truncating specific regions of FZD7, I was able to define regions essential for downstream signaling. By mapping the site where the Wnt mimetic binds FZD7, I was able to identify a short peptide region sufficient for Wnt mimetic binding. Incorporating this binding site into other FZD proteins renders them responsive to the FZD7-specific Wnt mimetic, thus providing a new avenue to specifically activate distinct FZD molecules.

MATERIALS AND METHODS:

Cell culture and stable line generation:

All transfections were performed in Human Embryonic Kidney (HEK) 293T FZD1,2,7 KO (3KO) SuperTopFlash (STF) cells (Butros lab). Cells were grown in 1x DMEM (Dulbecco's Modified Eagle's Medium, with high-glucose, L-glutamine, without sodium pyruvate) and 10% Fetal Bovine Serum. All transfections were done using Polyethylenimine (PEI) used at 1µg/µL, 1:4 ratio per 1µg of DNA, when cells were around 60% confluent. Immunoblotting and flow cytometry were done 48h post transfection. To generate stable cell lines, HEK293T 3KO STF cells were transfected with plasmid of interest, Blastcidin resistance and a piggyback transposase (to mediate stable integration of the piggyback plasmid into the genome (Mossine *et al.*, 2013) at a ratio of 9:1:1. PEI was used for transfection with the ratio of plasmid to PEI 1:4, for 1µg of DNA. 48h post transfection and thereafter, cells were cultured in 1xDMEM, 10% FBS and 8µg/mL Blasticidin S HCl. Transfected pools of cells were passaged after 72h of treatment with Blastcidin S HCL and allowed to grow to confluency in 6 well plates. Single cell colonies were established through serial dilution in 96 well plates, starting with 5000 cells/mL followed by serial dilution such that some wells receive only 1 cell. Single cells clones were identified about 2 weeks later as single colonies in individual wells of the 96-well plate. Some stable cell lines were generated with HEK293T 3KO cells. The cells were transfected with plasmid of interest, TopFlash cassette, Blastcidin resistance, Puromyocin resistance and piggyback transposase at a ratio of 9:9:1:1:1:1. PEI was used for transfection with the ratio of plasmid to PEI 1:4, for 1µg of DNA. 48h post transfection and thereafter, cells were cultured in 1xDMEM, 10% FBS, 8µg/mL Blasticidin S HCl and 4µg/mL puromyocin. Transfected pools of cells were passaged after 72h of treatment with Blastcidin S HCL and allowed to grow to confluency in 6 well plates. Single cell colonies were established as described above.

Plasmids:

Plasmid# pKW	Name	Expression vector	Resistance	Florophore
454	FZD7 L188 11AA TAPYLPDLPFT	Bacterial GST fusion	Amp	-
455	FZD7 L188 11AA YLPDLPFTALP	Bacterial GST fusion	Amp	-
475	FZD7 L188 8AA YLPDLPFT	Bacterial GST fusion	Amp	-
451	FZD7 TMD5-7	Mammalian	Amp	IRES-mKate
452	FZD7 TMD7	Mammalian	Amp	IRES-mKate
453	FZD7 TMD1	Mammalian	Amp	IRES-mKate
480	FZD2 V5	Mammalian	Amp	IRES-mKate
481	FZD9 V5	Mammalian	Amp	IRES-mKate
448	FZD7	Mammalian	Amp	IRES-mKate

449	FZD9	Mammalian	Amp	IRES-mKate
479	FZD2	Mammalian	Amp	IRES-mKate
466	FZD9-8aa V5	Mammalian	Amp	IRES-mKate
467	FZD9-8aa	Mammalian	Amp	IRES-mKate
474	FZD2-8aa V5	Mammalian	Amp	IRES-mKate
472	FZD2-8aa	Mammalian	Amp	IRES-mKate
490	FZD7 G551	Mammalian	Amp	IRES-mKate
491	FZD7 W551	Mammalian	Amp	IRES-mKate
492	FZD7 R559	Mammalian	Amp	IRES-mKate
494	Blast H2B-mTurquoise	Mammalian	Amp	H2B-mTurquoise
495	FZD9-V5 puro PB	Mammalian	Amp/Puro	-
496	FZD7 puro PB	Mammalian	Amp/Puro	-
497	FZD2 puro PB	Mammalian	Amp/Puro	-
498	FZD9 puro PB	Mammalian	Amp/Puro	-

499	FZD9-8aa puro PB	Mammalian	Amp/Puro	-
529	hFZD9 w/ hFZD7 ICL3	Mammalian	Amp	IRES-mKate
530	hFZD9 w/ hFZD7 CTT	Mammalian	Amp	IRES-mKate
531	hFZD7 w/ hFZD9 ICL3	Mammalian	Amp	IRES-mKate
532	hFZD7 w/ hFZD9 CTT	Mammalian	Amp	IRES-mKate
533	hFZD7 w/ hFZD9 CRD	Mammalian	Amp	IRES-mKate
450	hFZD9 w/ hFZD7 CRD	Mammalian	Amp	IRES-mKate
546	hFZD9 w/ hFZD7 ICL3 and CTT	Mammalian	Amp	IRES-mKate
560	hFZD7 w/ hFZD9 ICL3 and CTT	Mammalian	Amp	IRES-mKate

Immunoblotting:

Cells grown in 6 well plates at a 100% confluency, were washed in dPBS once and dissociated with cold dPBS. They were pelleted at maximum speed for 1 min. Cell pellets were resuspended in 100 µL RIPA lysis buffer (10mM Tris, pH 8.0, 1mM EDTA, 0.5mM EGTA, 1% Triton-x 100, 0.1% Sodium Deoxycholate, 0.1% SDS, 140mM NaCl) and protease inhibitor cocktail (Sigma protease inhibitor cocktail). Samples were placed on ice

for 30 min, inverting tubes at 10 min intervals. Samples were not heated. About 20 µg of total protein (as determined using a Bradford Assay [Bio-Rad Protein Assay Kit I-5000001])per lane was resolved by sodium dodecyl sulfate–polyacrylamide gel electrophoresis (SDS–PAGE), transferred to nitrocellulose, blocked for 1 h at room temperature in blocking buffer (TBS, 0.2% Tween-20, 1% BSA, 3% non-fat dry milk) and probed with the appropriate primary antibodies in blocking buffer overnight at 4 °C. Protein was detected following incubation with secondary antibodies for 1 h at room temperature, incubation with Western Lighting ECL Reagent (Fisher WBLUF0100), and exposure to autoradiography film. Primary antibodies used; αFZD7 (Fernandez et al. 2014), αFZD9 Rb 13865-1-AP Proteintech at a dilution of 1:2000, αV5 Mouse GTX628529 GeneTex used at 1:10000. Secondary Antibodies used- Goat anti-Human IgG Cross-Adsorbed Secondary Antibody, HRP, Thermofisher 62-8420 (1:15000). HRP Goat Anti-Rabbit IgG (H+L Chain Specific) Fisher 656120 (1:8000).

Expression of GST fusion proteins:

BL21 competent E.Coli were inoculated with the desired plasmid containing the sequence encoding various GST fusion proteins at 37°C, until the bacterial culture media reached OD_{600}=0.6. Following this, Isopropyl β- d-1-thiogalactopyranoside (IPTG) was added for a final concentration of 1mM and incubated for 4 h to induce expression of the GST fusion proteins. Bacteria were pelleted at 5000xg for 10 min at 4°C and the pellet was resuspended in cold PBS and protease inhibitor cocktail. The resuspended pellet was sonicated using on ice, 2 minutes, No pulse, 30%, 1/8" probe. The lysate was spun down at 15,000xg for 5 min at 4°C. The supernatant was filtered using a 0.22um syringe filter into a clean conical and stored at -80°C until use.

Dot blot:

2µL of the bacterial lysate containing the GST-fusion protein were spotted on a nitrocellulose membrane and dried. The membrane was blocked in blocking buffer (TBS, 0.2% Tween-20, 1% BSA, 3% non-fat dry milk) for 1 h. It was probed with anti-FZD7 antibody at 1 µg/mL for 1 h at room temperature, and washed thrice in TBST for 5 min. Protein was detected following incubation with secondary antibody (Goat anti-Human IgG Cross-Adsorbed Secondary Antibody, HRP, Thermofisher 62-8420 (1:15000)) for 1 h at room temperature and washed thrice in TBST for 5 min. It was incubated with Western Lighting ECL Reagent (Fisher WBLUF0100) and exposed to autoradiography film to detect protein as dots.

Flow Cytometry:

For transient transfections, cells in 6 well plates were transfected with 2µg DNA/well with PEI at 1µg/µL, 1:4 ratio per 1µg of DNA. 48 h post transfection, cells were dissociated with Accutase and blocked with FACS buffer (1 mM EDTA, 2% FBS, dPBS). They were stained with anti-FZD7 antibody at 1 µg/mL for 60 min, followed by a florescence conjugated secondary antibody for 30 min. Cells were also stained with DAPI. Florescence was measured on BLDSRFortessa and analyzed using FlowJo software. All images are presented post compensation for FITC and mKate.

Luciferase assay:

Stable cell lines were treated with Wnt3a or Wnt mimetic for 24h. Media was aspirated, and cells were lysed in luciferase lysis buffer (100mM K-PO_4 buffer, pH 7.8, 0.2% Triton X-100) for 15 minutes on a shaker at room temperature. 40 µL of buffer was added per well for a 96 well plate, 60 µL of buffer was added per well for a 24 well plate and 100µL of buffer was added per well of 12 well plate. 20µL of each sample was transferred to a white-

walled 96 well plate and assayed for luciferase activity. Reagents for the luciferase assay buffer: D-Luciferin-Potassium (BD 556877, 10mg) used at 10 mM, ATP (Sigma, A6419-10G) used at 0.25M, 0.25M Tris-Hcl, pH8, 1M $MgSO_4$. 100 µL luciferase buffer was added to each well containing samples and luciferase activity was quantified using a luminometer.

Results:

Epitope mapping:

An αhuman FZD7 antibody was generated by immunizing mice with solubilized membrane bound human FZD7. Following this, an antibody engineered from a bacterially produced antigen binding fragment (Fab) was isolated (Fernandez et al., 2014) and a monoclonal hFZD7 antibody (F7) was generated. Mapping the site of binding of F7 on FZD7 was made possible by the fact that F7 recognizes human FZD7, but not mouse Fzd7. hFZD7 and mFzd7 differ only in the region between the CRD and the first TM (Figure 1). This region contains the complete epitope of 41 amino acids (SGGPGGGPTAYPTAPYLPDLPFTALPPGASDGRGRPAFPFS) with mFzd7 differing in 7 amino acids. This suggests that changing one or more of these 7 amino acids in mFzd7 would confer F7 binding (Figure 2A). When the mouse proline residue at position 188 is mutated to a leucine (Fzd7-P188L), F7 can then recognize the mouse Fzd7 protein. Alternatively, when the human leucine residue at position 188 is mutated to a proline (FZD7-L188P) results in F7 no longer recognizing the protein, demonstrating that L188 residue is essential for F7 recognition of the FZD7 protein (Gumber *et al.*, manuscript in preparation).

To identify the minimal FZD7 sequence required for F7 binding, we generated a fusion protein between GST and the 41 amino acid sequence that includes L188 and tested its reactivity with F7 using a dot blot (Figure 2B). As expected, F7 binds to this GST fusion protein. The full-length epitope of 41 amino acids (AA) (SGGPGGGPTAYPTAPYLPDLPFTALPPGASDGRGRPAFPFS) was shortened by removing amino acids from either end, keeping Leu position 188 constant. The epitope was shortened to two different versions containing 11 AA and finally shortened to be YLPD**L**PFT, 8 amino acids long (Figure 2C). These GST-fusion proteins were then expressed in bacteria. A dot blot was performed using F7 on cell lysates isolated from

bacteria expressing the full-length epitope (41 AA), the full-length epitope containing L188P mutation, an uninduced control, the two 11 AA versions and the shortest epitope at 8 AA. As expected, F7 antibody recognized the full-length epitope sequence and did not recognize the full-length epitope containing a L188P mutation. Lysates from bacteria not induced to express the GST-fusion proteins were not reactive with F7. The F7 antibody recognized and bound to both 11AA versions of the epitope (TAPYLPDLPFTALP, TAPYLPDLPFT) as well as the shortest epitope length of 8AA (YLPDLPFT) (Figure 2D). Therefore, the epitope region of F7 maps to an 8 AA extracellular portion in FZD7. Further BLASTP analysis against nonredundant protein sequences in homo sapiens using the 8AA epitope yielded no 100% identity matches except in human FZD7. The remaining matches were to proteins that were intracellular. Since we use F7 and its derivative Wnt mimetic to bind FZD7 on the cell surface, these distantly related proteins are unlikely to react with F7 or the WNT mimetic (Figure 2E). The shortened 8AA (YLPD**L**PFT) epitope is recognized by the monoclonal F7, and this sequence is unique to FZD7.

Activation of specific FZD receptors:

In the Willert lab, a bispecific protein, the Wnt mimetic, was created by fusing a single chain variable fragment (scFv) derived from F7 to and scFv derived from a publicly available LRP6 antibody. Due to its ability to simultaneously bind to FZD7 and LRP6, the Wnt mimetic functions as a Wnt agonist by forcing the heterodimerization of the two cell surface receptors resulting in the activation of the β-catenin dependant Wnt signalling cascade. The Wnt mimetic is highly specific to FZD7 and will only elicit a Wnt response in cells that express FZD7 on the cell membrane.

We wanted to extend the signalling specificity of the Wnt mimetic by testing whether the addition of shortened 8AA (YLPD**L**PFT) epitope, which is recognized by F7, could

confer binding specificity and activation of other FZD receptors. Aligning all FZDs and creating a phylogenetic tree showed that FZD2 was closely related to FZD7, which indicated that they are likely to have similar structures (Figure 3A). As a result, it makes it a good candidate for tagging as the addition of the 8 AA tag is less likely to disrupt its folding or activity. We also chose FZD9 for such a tagging experiment because FZD9 signals with Wnt9A to regulate blood development (Grainger et al. 2019), however active Wnt9A has not been purified. To work around this, FZD9 was to be tagged with the 8AA sequence so that it can be activated with F7L6 independently of its Wnt ligand (Figure 3A). Further sequence alignment of all FZDs between the CRD and first transmembrane domain, shows that the 8AA epitope region from FZD7 is not conserved in other FZDs (Figure 3B). The 8AA sequence was added to FZD2 between A188 and P189 residues, mimicking the location of the 8AA sequence in FZD7 (Figure 3C). Previous iterations of adding the F7 epitope in the region between the CRD and first transmembrane domain of zebrafish Fzd9b resulted in F7 being unable to recognize and bind to the sequence (data not shown). The reason for the lack of reactivity of F7 with this tagged Zebrafish Fzd9b is unknown, however, we speculate that in this context this short 8 AA epitope is inaccessible to F7. To work around this, the 8AA tag was placed right after the signal sequence and before the CRD in FZD9, as seen in the schematic (Figure 3C). V5-tagged versions of FZD2, FZD7, FZD9 and FZD2-8AA tag were generated. These constructs were transiently expressed on the surface of HEK293T3KO cells and probed with F7. FZD7 was recognized and so were the tagged FZD receptors, but not FZD9 and FZD2 (Figure 3D).

Stable cell lines were generated using HEK293T FZD1,2,7 KO SuperTopFlash (3KO-STF) cell line. The expression of the FZD constructs and the ability of F7 to recognize them was analyzed by immunoblotting. A western blot was conducted to test whether F7 was able to recognize the 8AA epitope region when the tagged FZDs were stably expressed. The blot

was probed with F7 and contained transiently expressed wildtype FZD7 as a control. F7 recognized FZD7, FZD2-8AA tag, FZD9-8AA tag but not FZD9 and FZD2 (Figure 4A). This shows that the shortened epitope region can still be recognized in the area that it was inserted in FZD2 and FZD9, and that this binding is unique to the tagged FZDs. Furthermore, it shows that the cell lines stably express this construct, which allows for the line to be tested further.

Since protein modifications, such as tagging, can render a protein inactive, we wanted to ensure that the tagged FZDs and FZD7 in our cell lines were expressed on the cell surface. To test this, flow cytometry was performed on non-permeabilized cells using F7 to detect the FZD proteins on the cell surface. The F7 antibody binding to the FZD transgenes was detected with a FITC-conjugated secondary antibody. As expected, untransfected cells were not recognized by F7. Cells expressing either FZD7, FZD2-8AA tag and FZD9-8AA tag were effectively stained with F7, confirming that these proteins were present on the cell surface (Figure 4B). This confirms that not only are constructs being stably expressed, they are also being trafficked to the cell surface. This will now allow us to test if these constructs can be activated by the Wnt mimetic as they contain the epitope binding region of F7 and are on the cell surface.

A luciferase assay was conducted with the following stable lines in HEK293 3KO-STF cells; FZD7, FZD2, FZD9, FZD2-8AA tag, FZD9-8AA tag (Figure 4C). As expected FZD7 had signaling activity with both Wnt3a and Wnt mimetic. Signaling activity in FZD2 was only induced with Wnt3a conditioned media, as Wnt3a signals through FZD2 (Voloshanenko et al., 2017). As expected, the Wnt mimetic did not induce any signaling activity through FZD2. The FZD2 tagged with the 8AA epitope was activated through both Wnt3a and the Wnt mimetic. FZD2-8AA tag exhibited an 8-fold increase in activation with the Wnt mimetic compared to untreated conditioned media. FZD9 was activated by the Wnt3a conditioned media, but not through the Wnt mimetic conditioned media. FZD9-8AA

tag was activated by both the Wnt3a and Wnt mimetic conditioned media, where the Wnt mimetic conditioned media activated FZD9-8AA by 10-fold (Figure 4C). These experiments demonstrate that tagging other FZDs, in this case FZD2 and FZD9, with the 8AA tag derived from FZD7 renders them signalling competent to the WNT mimetic. Therefore, heterodimerization of several FZDs (FZD2, 7 and 9) with LRP6 is sufficient to activate Wnt/β-catenin signaling.

FZD7 containing tail truncations and transmembrane domain deletions:

Previous experiments in the lab using the Wnt mimetic showed that FZD7's CRD was not required to mediate intracellular β-catenin signaling (data not shown). This pointed to the TM domains and intracellular components of FZD7 mediating signaling. To test which regions of FZD7 were sufficient for signaling, several constructs of FZD7 were generated. Three constructs containing transmembrane domain deletions were generated; FZD7 with transmembrane domain 1 and the C-terminal tail (FZD7-TM1), FZD7 with transmembrane domain 7 and the C-terminal tail (FZD7-TM7), and FZD7 with transmembrane domains 5-7 and the C-terminal tail (FZD7 TM5-6) (Figure 5A). Another three constructs with different lengths of the C-terminal tail (CTT) were generated ending at G551, W557, R559 respectively (Figure 5A). Expression of these constructs in HEK293T 3KO cells was verified through western blotting with F7. As expected, the transmembrane domain deletion constructs were smaller in size than FZD7 as revealed by their faster mobility on denaturing polyacrylamide gel. The tail truncations, which lack only a few AA, migrated at a similar position to FZD7 (Figure 5B). All FZD7 constructs were detected by immunoblotting, indicated that the truncated proteins were expressed.

Following this, flow cytometry was performed to ascertain if the FZD7 constructs were being expressed on the cell surface. All constructs contain an IRES mKate so that

transfected cells could be readily detected. FZD7 TM1, FZD7 TM7 and FZD7 TM5-7 were not detected on the cell surface (Figure 5C), suggesting that they may not be folded properly to permit their transit through the secretory pathway. In contrast, FZD7 W551, FZD7 W557 and FZD7 R559 were expressed on the cell surface (Figure 5C). As the transmembrane domain deletion constructs were not being trafficked to the cell surface, their interaction with signaling molecules and subsequent signaling ability cannot be tested. This shows that the presence of transmembrane domains is necessary for the proper trafficking of the protein to the cell surface, while shortening of the CTT did not affect its trafficking to the cell surface.

The tail truncation FZD7 constructs were transfected into HEK293T 3KO-STF cells, which are non-responsive to Wnt3a. Stable cell lines containing FZD7, FZD7 G551 and FZD7 W557 were successfully generated by selection in Blasticidin (Figure 6A). Protein expression was verified through a western blot probing for FZD7 (Figure 6B) with F7. To test their signaling abilities, cell lines were treated with Wnt3a condition media from CHO cells for 24 hours and a luciferase assay was conducted. Cells expressing FZD7 had nearly a 900-fold activation of STF activity while FZD7 G551 and FZD7 W557 had around a 4-fold activation (Figure 6C), indicating that the C-terminal tail of FZD7 plays a role in β-catenin dependent signaling.

FZD7 and FZD9 Swaps:

To further understand which regions of FZD7 are important for signaling, several swaps between FZD7 and FZD9 were generated. Wnt3a effectively signals through FZD7. At the time that we designed these swapping experiments, we selected FZD9 for these domain swapping experiments because Voloshanenko et al. reported that FZD9 did not appreciably transduce the Wnt3a signaled (2017). However, we observed that FZD9 couples to Wnt3a at equivalent levels as FZD7 does (see Figure 4c). FZD7 containing FZD9 intracellular loop 3

(FZD7 ICL3-S), FZD7 containing FZD9 C-terminal tail (FZD7 CTT-S), FZD7 containing FZD9 intracellular loop 3 and C-terminal tail (FZD7 ICL3,CTT-S) and FZD9 containing FZD7 CRD and 1st extracellular domain (FZD9 CRD-S) were generated (Figure 7A). These constructs were expressed in HEK 293T 3KO cell lines and protein expression was verified using a western blot probed with αhFZD7 antibody. FZD7 ICL3-S, FZD7 CTT-S and FZD7 ICL3,CTT-S were expressed in the cells however, FZD9 CRD-S was not expressed (Figure 7B). To verify cell surface expression, flow cytometry was performed with the αhFZD7 antibody. Only FZD7 ICL3-S, FZD7 CTT-S and FZD7 ICL3, CTT-S were expressed on the cell surface membrane (Figure 7C).

Similar swaps were conducted with FZD9. FZD9 containing FZD7 intracellular loop 3 (FZD9 ICL3-S), FZD9 containing FZD7 C-terminal tail (FZD9 CTT-S), FZD9 containing FZD7 intracellular loop 3 and C-terminal tail (FZD9 ICL3,CTT-S) and FZD7 containing FZD9 CRD and 1st extracellular domain (FZD7 CRD-S) were generated (figure 8A). These constructs were expressed in HEK 293T 3KO cell lines and protein expression was verified using a western blot probed with αhFZD9 antibody. FZD9 ICL3-S, FZD9 CTT-S and FZD9 ICL3,CTT-S and FZD7 CRD-S were expressed (Figure 8B).

Discussion:

FZD7 containing tail truncations and transmembrane domain deletions:

Previous experiments in the lab have shown that the CRD of FZD7 is not required for β-catenin dependent signaling (Gumber et al., manuscript in preparation). Through a Wnt reporter assay, called Super Top-Flash (STF), it was shown that F7L6, a Wnt mimetic, was able to activate signaling even when FZD7's CRD was removed as long as the transmembrane proximal region, which contains the binding site for F7L6, remained. This observation points to other components of FZD7 mediating signaling. The generation of transmembrane domain deletions and tail truncations in FZD7 showed that deleting transmembrane domains prevented those constructs from being trafficked to the cell surface. FZD7 containing tail truncations, FZD7 G551 and FZD7W557 were trafficked to the cell surface. However, when treated with Wnt3a condition media, both these constructs had drastically reduced signaling ability compared to WT FZD7 with the full length of the tail. The reduction in signaling ability of FZD7 G551 which does not contain a KTXXXW motif, is consistent with previous findings in *Xenopus* Fz3 and Fz7, mutations in the conserved KTXXXW motif resulted in a loss of signaling activity (Umbhauer *et al.*,2000). The function of KTXXW motif is likely conserved in human FZDs, as seen in FZD7 W551. FZD7 W557 contains and ends at the KTXXXW motif, and it also exhibited reduced signaling ability compared to WT FZD7. This is consistent with mouse FZD4, as it also requires distal amino acids to the KTXXXW motif to efficiently signal through the tcf/lef pathway using Norrin (Bertalovitz *et al.*,2016). This suggests the secondary structure of the FZD C-terminal tail is changed, which impairs its ability to interact or recruit other signaling molecules for downstream activation of the TCF/LEF pathway. In canonical signaling, the binding of DVL to the intracellular components of the FZD receptor is known to be an important event (Macdonald et al., 2010). However, there have been conflicting observations of where

Dishevelled interacts with the FZD receptor. Wong et al., observed that DVL binds to the KTXXXW motif in the C-terminal tail of the Fzd receptor in Xenopus and Drosophilia (2003). On the other hand, Tauriello et al., observed that Dishevelled, and other proteins involved in the signaling pathway, interact with the third intercellular loop and C-terminal tail of mouse Fzd5 (Tauriello et al., 2012). However, we do not yet know which regions of Human FZD7 are required for interactions with DVL and other proteins involved in the pathway. Perhaps the loss of distal amino acids in the C-terminal tail of FZD7 is impairing its recruitment of important signaling molecules, explaining the reduced signaling activity.

Future directions include assaying for different protein interactions with the c-terminal tail and mutating amino acid residues to understand how the tail of FZD7 functions in terms of signaling.

FZD7 and FZD9 swaps:

Grainger and colleagues studied hemopoietic stem cell development in zebrafish and uncovered a highly specific interaction between Fzd9b and Wnt9a (Grainger et al., 2019). Using a series of chimeric Fzd receptors, they identified that specific regions of Fzd9b were critical in conferring Wnt9a signaling specificity. They swapped domains of two zebrafish Fzd receptors, one which signaled strongly through zebrafish Wnt9a and one which had poor signaling activity. It was found that the third intracellular loop (ICL3) and C-terminal tail (CTT) conferred signaling ability through domain swaps of these Fzds (Grainger *et al.*, 2019). This suggested that there was an interaction in this region which mediated the signaling specificity between Wnt9a and Fzd9b. We aimed to find a similar region in FZD7 that conferred signaling ability through Wnt3a and potentially finding regions that mediate intracellular signaling. The next steps would be to generate stable cell lines expressing these chimeric constructs in HEK293T 3KO S-TF cells and test for signaling ability with Wnt3a.

Analysis of this data can lead to the potential elucidation of regions of FZD7 that might be specific to its function.

Epitope mapping and FZD activation:

Most Wnts are not available in a soluble form, making it difficult to activate specific receptors to study their signaling pathway (Mulligan *et al.*, 2011). The use of the Wnt mimetic F7L6 and the FZD7 epitope as a tag circumvents this issue. By shortening the 41 amino acid epitope to 8 amino acids, and retaining the binding specificity of the αhumanFZD7 antibody (F7), we demonstrated that a short peptide sequence is sufficient for F7 binding.

Mapping the epitope of F7 showed that it was a linear string of amino acids which was surprising since many epitopes are often comprised of several regions of the protein that are brought together when the protein folds into its 3-dimensional structure. Since the epitope is a linear string of amino acids, F7 is still able to bind to and recognize the epitope when the protein structure is denatured as its binding is not dependent on the final conformation of the protein. The sequential shortening of the epitope allowed the epitope to be recognized by F7, even when it was only 8AA in length. Conducting a BLAST analysis of the 8AA sequence against the human proteome showed that this sequence is not perfectly matched anywhere except in the human FZD7 protein and any other similar matches were in intracellular proteins. As a result, this 8AA epitope has great utility as a tag for other FZDs or other proteins to measure expression levels. Furthermore, this tag along with F7 may prove useful for purification of recombinant proteins.

The tagging of other FZD receptors with the 8AA tag allowed for recognition and binding by F7. The Wnt mimetic developed in the Willert lab is comprised of two scFvs, one that binds FZD7 (and derived from the antibody F7) and one that binds LRP6. Addition of

the Wnt mimetic to cells expressing FZD7 and LRP6 leads to their heterodimerization and subsequent β-catenin dependent signaling (Gumber *et al.,* Manuscript in preparation). Combining the FZD receptors tagged with the 8AA sequence and the Wnt mimetic provides an avenue for specific activation of these receptors through a Wnt independent manner. This allowed for the heterodimerization of the FZD receptors and LRP6, activating signaling. Given the lack of Wnt/FZD specificity having a Wnt mimetic that is extremely specific to just FZD7 makes it extremely unique. Similar Wnt mimetics have been engineered by others, however, these Wnt agonists engaged miultiple FZDs (Janda *et al.,* 2017). Other FZD-LRP binding antibodies that act as Wnt agonists have a broad specificity targeting FZD1,2,4,5 7 and 8 (Tao *et al.,*2017). The Wnt mimetic in our lab differs in that it is extremely specific to the epitope region on FZD7 and does not have cross reactivity. Furthermore, we have shown that the Wnt mimetic can be sensitized to FZD receptors. This allows us to use this as a highly specific tool to activate specific FZD receptors that have been tagged with the shortened amino acid sequence.

Now that we have shown that the Wnt mimetic in the lab can be sensitized to other FZD receptors, this tool can be extended further to study downstream signaling of these receptors. It would be interesting to study the genes that are activated through the Wnt mimetic and comparing it to activation of genes when the receptor is activated by endogenous Wnt ligands. Furthermore, given that FZD9 is involved in hematopoiesis, the tagged FZD9 receptor and Wnt mimetic could potentially be used to drive this differentiation.

References:

Bertalovitz, A. C., Pau, M. S., Gao, S., Malbon, C. C., & Wang, H. Y. (2016). Frizzled-4 C-terminus Distal to KTXXXW Motif is Essential for Normal Dishevelled Recruitment and Norrin-stimulated Activation of Lef/Tcf-dependent Transcriptional Activation. *Journal of molecular signaling*, *11*, 1. https://doi.org/10.5334/1750-2187-11-1

Cao, T. T., Xiang, D., Liu, B. L., Huang, T. X., Tan, B. B., Zeng, C. M., Wang, Z. Y., Ming, X. Y., Zhang, L. Y., Jin, G., Li, F., Wu, J. L., Guan, X. Y., Lu, D., & Fu, L. (2017). FZD7 is a novel prognostic marker and promotes tumor metastasis via WNT and EMT signaling pathways in esophageal squamous cell carcinoma. *Oncotarget*, *8*(39), 65957–65968. https://doi.org/10.18632/oncotarget.19586

Chang, H., Smallwood, P. M., Williams, J., & Nathans, J. (2016). The spatio-temporal domains of Frizzled6 action in planar polarity control of hair follicle orientation. *Developmental biology*, *409*(1), 181–193. doi:10.1016/j.ydbio.2015.10.027

Croce, J. C., & McClay, D. R. (2008). Evolution of the Wnt pathways. *Methods in molecular biology (Clifton, N.J.)*, *469*, 3–18. doi:10.1007/978-1-60327-469-2_1

Dann, C. E., Hsieh, J.-C., Rattner, A., Sharma, D., Nathans, J., & Leahy, D. J. (2001). Insights into Wnt binding and signalling from the structures of two Frizzled cysteine-rich domains. Nature, 412(6842), 86–90. doi: 10.1038/35083601

Dijksterhuis, J. P., Baljinnyam, B., Stanger, K., Sercan, H. O., Ji, Y., Andres, O., Rubin, JS., Hannoush, RN., Schulte, G. (2015). Systematic mapping of WNT-FZD protein interactions reveals functional selectivity by distinct WNT-FZD pairs. The Journal of biological chemistry, 290(11), 6789–6798. doi:10.1074/jbc.M114.612648

Fernandez, A., Huggins, I. J., Perna, L., Brafman, D., Lu, D., Yao, S., Gaasterland, T., Carson, D. A., & Willert, K. (2014). The WNT receptor FZD7 is required for maintenance of the pluripotent state in human embryonic stem cells. *Proceedings of the National Academy of Sciences of the United States of America*, *111*(4), 1409–1414. https://doi.org/10.1073/pnas.1323697111

Grainger, S., Nguyen, N., Richter, J., Setayesh, J., Lonquich, B., Oon, C. H., Wozniak, JM., Barahona, R., Kamei, CN., Houston, J., Carrillo-Terrazas, M., Drummond, IA., Gonzalez, D., Willert, K., Traver, D. (2019). EGFR is required for Wnt9a-Fzd9b signalling specificity in haematopoietic stem cells. Nature cell biology, 21(6), 721–730. doi:10.1038/s41556-019-0330-5

Gurney A, Axelrod F, Bond CJ, Cain J, Chartier C, Donigan L, Fischer M, Chaudhari A, Ji M, Kapoun AM, Lam A, Lazetic S, Ma S, Mitra S, Park IK, Pickell K, Sato A, Satyal S, Stroud M, Tran H, Yen WC, Lewicki J, Hoey T. (2012). Wnt pathway inhibition via the targeting of Frizzled receptors results in decreased growth and tumorigenicity of human tumors. *Proceedings of the National Academy of Sciences of the United States of America*, *109*(29), 11717–11722. https://doi.org/10.1073/pnas.1120068109

Janda, C. Y., Waghray, D., Levin, A. M., Thomas, C., & Garcia, K. C. (2012). Structural basis of Wnt recognition by Frizzled. *Science (New York, N.Y.)*, *337*(6090), 59–64. https://doi.org/10.1126/science.1222879

Kirikoshi, H., Sekihara, H., & Katoh, M. (2001). Up-regulation of Frizzled-7 (FZD7) in human gastric cancer. International Journal of Oncology. doi: 10.3892/ijo.19.1.111

Komiya, Y., & Habas, R. (2008). Wnt signal transduction pathways. Organogenesis, 4(2), 68–75. doi:10.4161/org.4.2.5851

MacDonald, B. T., Tamai, K., & He, X. (2009). Wnt/beta-catenin signaling: components, mechanisms, and diseases. Developmental cell, 17(1), 9–26. doi:10.1016/j.devcel.2009.06.016

Mardones, M.D., Andaur, G.A., Varas-Godoy, M. *et al.* Frizzled-1 receptor regulates adult hippocampal neurogenesis. *Mol Brain* **9,** 29 (2016). https://doi.org/10.1186/s13041-016-0209-3

Martyn, I., Kanno, T. Y., Ruzo, A., Siggia, E. D., & Brivanlou, A. H. (2018). Self-organization of a human organizer by combined Wnt and Nodal signalling. *Nature*, *558*(7708), 132–135. doi:10.1038/s41586-018-0150-y

Miller J. R. (2002). The Wnts. Genome biology, 3(1), REVIEWS3001. doi:10.1186/gb-2001-3-1-reviews3001

Mossine, V. V., Waters, J. K., Hannink, M., & Mawhinney, T. P. (2013). piggyBac transposon plus insulators overcome epigenetic silencing to provide for stable signaling pathway reporter cell lines. *PloS one*, *8*(12), e85494. https://doi.org/10.1371/journal.pone.0085494

Mulligan, K. A., Fuerer, C., Ching, W., Fish, M., Willert, K., & Nusse, R. (2011). Secreted Wingless-interacting molecule (Swim) promotes long-range signaling by maintaining Wingless solubility. Proceedings of the National Academy of Sciences, 109(2), 370–377. doi: 10.1073/pnas.1119197109

Nusse, Roel. "Wnt Signaling in Disease and in Development." *Cell Research*, vol. 15, no. 1, 2005, pp. 28–32., doi:10.1038/sj.cr.7290260.

Qi J, Yu Y, Akilli Ozturk O, Holland JD, Besser D, Fritzmann J, Wulf-Goldenberg A, Eckert K, Fichtner I, Birchmeier W. New Wnt/beta-catenin target genes promote experimental metastasis and migration of colorectal cancer cells through different signals. Gut. 2016;65:1690–1701

Reya, T., & Clevers, H. (2005). Wnt signalling in stem cells and cancer. Nature, 434(7035), 843–850. doi: 10.1038/nature03319

Ring, L., Neth, P., Weber, C., Steffens, S., & Faussner, A. (2014). β-Catenin-dependent pathway activation by both promiscuous "canonical" WNT3a–, and specific "noncanonical" WNT4– and WNT5a–FZD receptor combinations with strong differences in LRP5 and LRP6 dependency. Cellular Signalling, 26(2), 260–267. doi: 10.1016/j.cellsig.2013.11.021

Sagara, N., Toda, G., Hirai, M., Terada, M., & Katoh, M. (1998). Molecular Cloning, Differential Expression, and Chromosomal Localization of HumanFrizzled-1, Frizzled-2,andFrizzled-7. Biochemical and Biophysical Research Communications, 252(1), 117–122. doi: 10.1006/bbrc.1998.9607

Stenman, J. M., Rajagopal, J., Carroll, T. J., Ishibashi, M., Mcmahon, J., & Mcmahon, A. P. (2008). Canonical Wnt Signaling Regulates Organ-Specific Assembly and Differentiation of CNS Vasculature. Science, 322(5905), 1247–1250. doi: 10.1126/science.1164594

Tamai K, Semenov M, Kato Y, Spokony R, Liu C, Katsuyama Y, Hess F, Saint-Jeannet JP, He X. 2000. LDL-receptor-related proteins in Wnt signal transduction. Nature 407: 530–35

Tanaka, S., Akiyoshi, T., Mori, M., Wands, J. R., & Sugimachi, K. (1998). A novel frizzled gene identified in human esophageal carcinoma mediates APC/beta-catenin signals. Proceedings of the National Academy of Sciences of the United States of America, 95(17), 10164–10169. doi:10.1073/pnas.95.17.10164

Tauriello, D. V., Jordens, I., Kirchner, K., Slootstra, J. W., Kruitwagen, T., Bouwman, B. A., Noutsou, M., Rüdiger, S. G., Schwamborn, K., Schambony, A., & Maurice, M. M. (2012). Wnt/β-catenin signaling requires interaction of the Dishevelled DEP domain and C terminus with a discontinuous motif in Frizzled. *Proceedings of the National Academy of Sciences of the United States of America*, *109*(14), E812–E820. https://doi.org/10.1073/pnas.1114802109

Tsukamoto AS, Grosschedl R, Guzman RC, Parslow T, Varmus HE. Expression of the int-1 gene in transgenic mice is associated with mammary gland hyperplasia and adenocarcinomas in male and female mice. Cell 1988; 55: 619–625

Ueno, K., Hazama, S., Mitomori, S., Nishioka, M., Suehiro, Y., Hirata, H., Oka, M., Imai, K., Dahiya, R., Hinoda, Y. (2009). Down-regulation of frizzled-7 expression decreases survival, invasion and metastatic capabilities of colon cancer cells. British journal of cancer, 101(8), 1374–1381. doi:10.1038/sj.bjc.6605307

Umbhauer, M., Djiane, A., Goisset, C., Penzo-Méndez, A., Riou, J. F., Boucaut, J. C., & Shi, D. L. (2000). The C-terminal cytoplasmic Lys-thr-X-X-X-Trp motif in frizzled receptors mediates Wnt/beta-catenin signalling. The EMBO journal, 19(18), 4944–4954. doi:10.1093/emboj/19.18.4944

Voloshanenko, O., Gmach, P., Winter, J., Kranz, D., & Boutros, M. (2017). Mapping of Wnt-Frizzled interactions by multiplex CRISPR targeting of receptor gene families. *FASEB journal : official publication of the Federation of American Societies for Experimental Biology*, *31*(11), 4832–4844. https://doi.org/10.1096/fj.201700144R

Wang, Y., Chang, H., Rattner, A., & Nathans, J. (2016). Frizzled Receptors in Development and Disease. *Current topics in developmental biology*, *117*, 113–139. doi:10.1016/bs.ctdb.2015.11.028

Willert, K., Brown, J., Danenberg, E., Duncan, A., Weissman, I., & Reya, T., Yate JR 3rd, Nusse, R.. (2003). Wnt proteins are lipid-modified and can act as stem cell growth factors. Nature, 423(6938), 448-452. doi: 10.1038/nature01611

Willert, K., & Nusse, R. (2012). Wnt proteins. *Cold Spring Harbor perspectives in biology*, *4*(9), a007864. https://doi.org/10.1101/cshperspect.a007864

Wong, H. C., Bourdelas, A., Krauss, A., Lee, H. J., Shao, Y., Wu, D., Mlodzik, M., Shi, D. L., & Zheng, J. (2003). Direct binding of the PDZ domain of Dishevelled to a conserved internal sequence in the C-terminal region of Frizzled. *Molecular cell*, *12*(5), 1251–1260. https://doi.org/10.1016/s1097-2765(03)00427-1

Yu, H., Ye, X., Guo, N., & Nathans, J. (2012). Frizzled 2 and frizzled 7 function redundantly in convergent extension and closure of the ventricular septum and palate: evidence for a network of interacting genes. *Development (Cambridge, England)*, *139*(23), 4383–4394. https://doi.org/10.1242/dev.083352

Zhang, W., Lu, W., Ananthan, S., Suto, M. J., & Li, Y. (2017). Discovery of novel frizzled-7 inhibitors by targeting the receptor's transmembrane domain. *Oncotarget*, *8*(53), 91459–91470. https://doi.org/10.18632/oncotarget.20665

Zimmerman, Z. F., Moon, R. T., & Chien, A. J. (2012). Targeting Wnt pathways in disease. *Cold Spring Harbor perspectives in biology*, *4*(11), a008086. https://doi.org/10.1101/cshperspect.a008086

Figures:
1

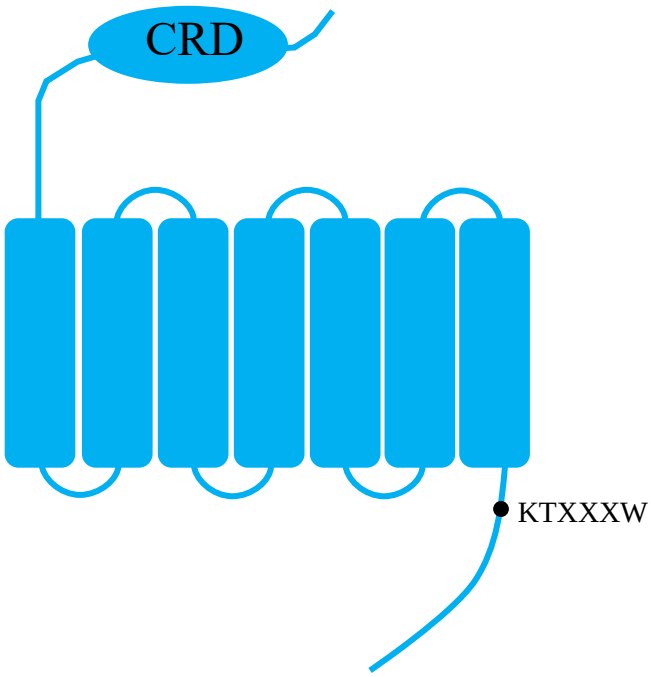

Figure 1: Schematic of FZD7, a 7 pass transmembrane domain receptor. The cysteine rich domain (CRD) of FZD7 is located in the extracellular portion of the cell and is required for Wnt ligand binding. FZD7 has 7 transmembrane domains and a c-terminal tail (CTT). The CTT contains a conserved motif "K-T-X-X-X-W" which is important in recruiting proteins to the cell surface for β-catenin dependent signaling.

2

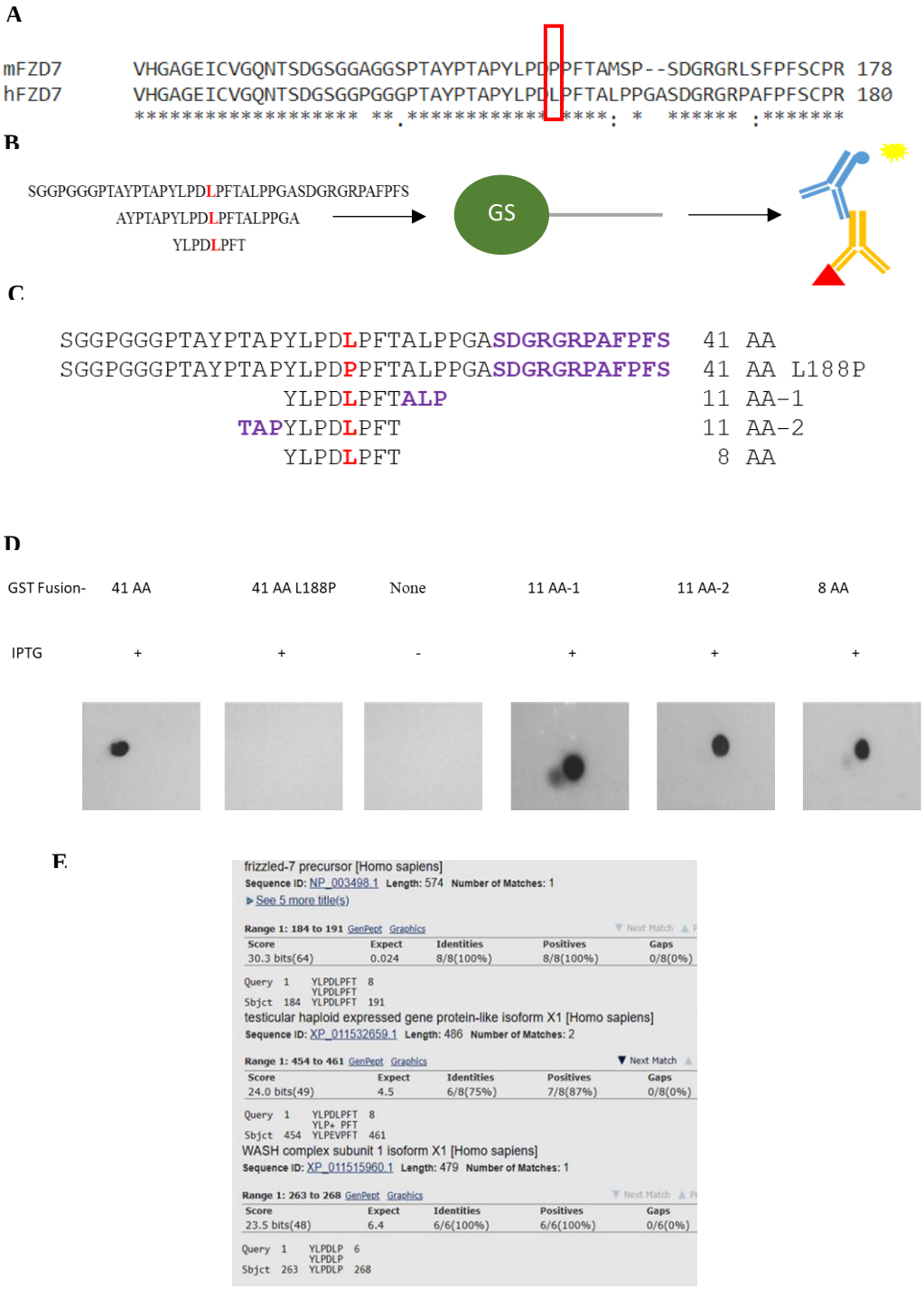

Figure 2: Identifying an epitope region of FZD7 specific to the αFZD7 portion of the Wnt mimetic. A: Creating a point mutation L188P causes α FZD7 (F7) to not recognize the full length epitope. B: Schematic of shortening the epitope region, expression and immunoblotting. C: Amino acids removed from either side of Leucine position 188. D: Dot blot containing lysates prepared from bacteria expressing labelled constructs blotted against αFZD7 antibody. E: BLASTP analysis against the human proteasome revealing the shortened epitope is unique to FZD7 and any other similar sequences are found intracellularly.

3

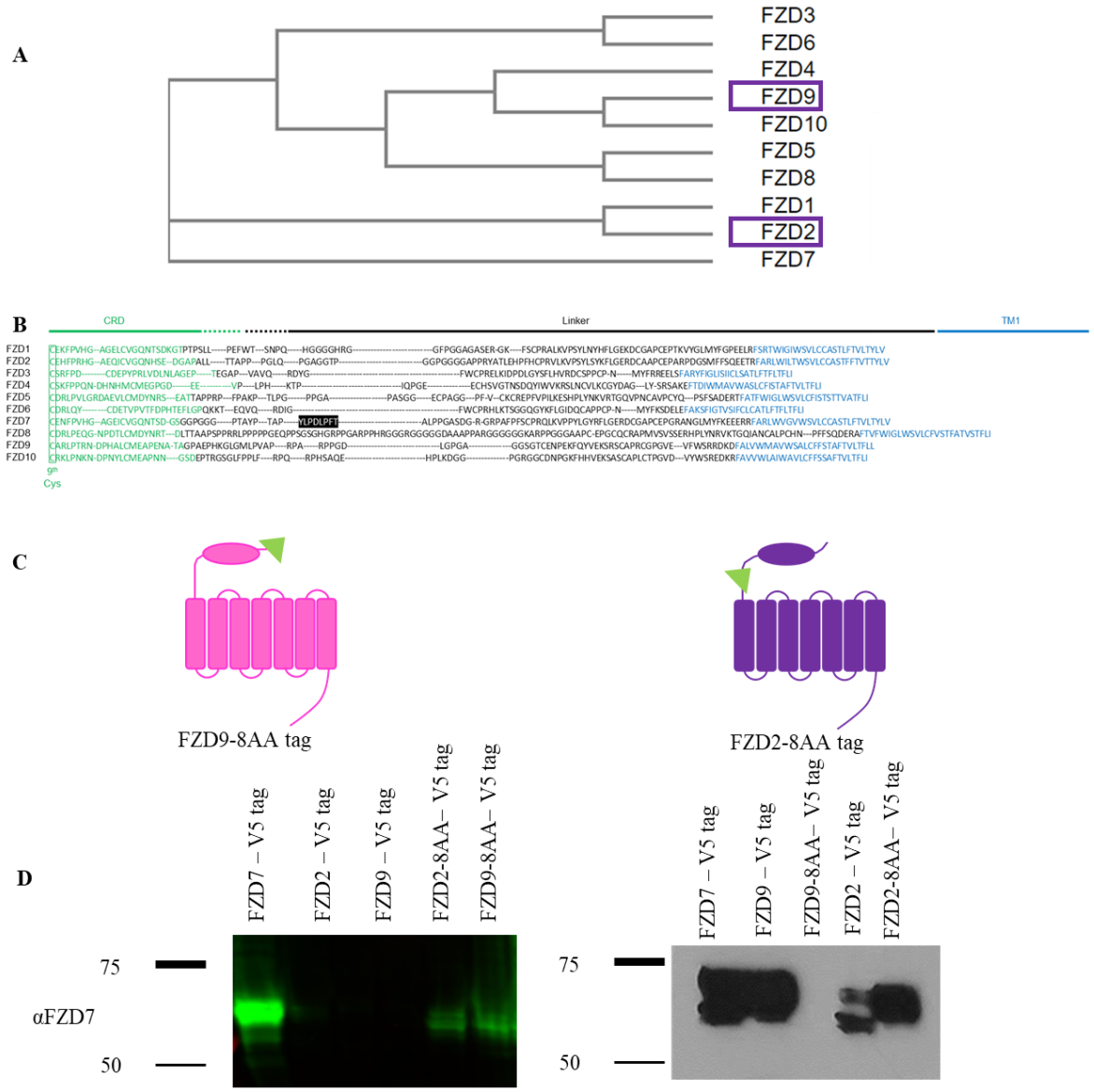

Figure 3: Construct design of tagged FZDs. A: Phylogentic tree of 10 human FZDs.B: Amino acid alignment of 10 human FZDs of the region between the cysteine rich region and the first transmembrane domain. C: Schematic of plasmid design for FZD9 tagged with the 8AA epitope and FZD2 tagged with the 8AA epitope, the epitope is represented as a green triangle. D: Western blot of FZD7-V5 tag, FZD2-V5 tag, FZD9-V5 tag, FZD2-8AA-V5 tag, FZD9-8AA-V5 tag, probed for both FZD7 and V5.

4

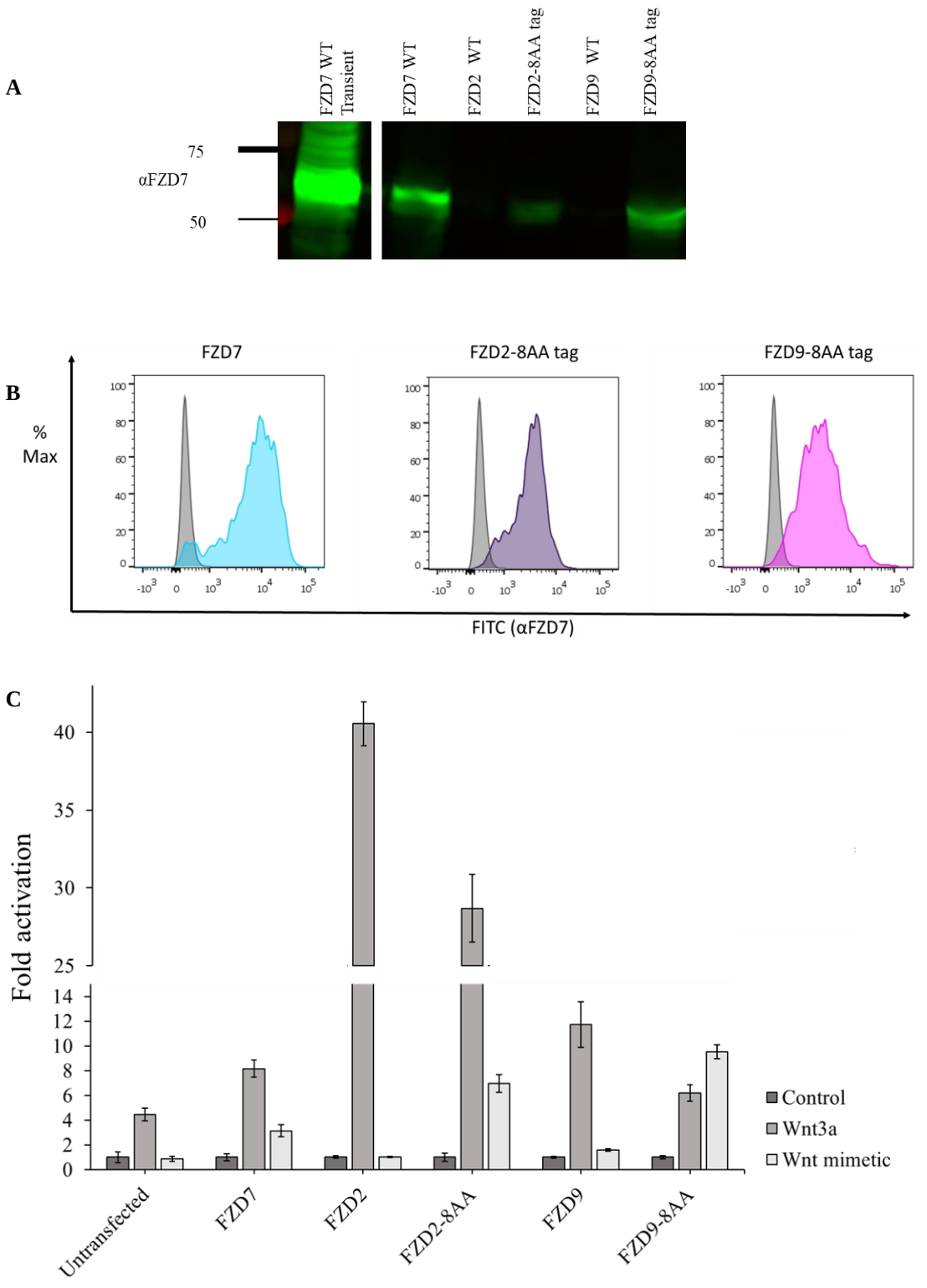

Figure 4: Generation and expression of stable cell lines containing FZDs with the epitope tag. A: Western blot of the stable lines of the tagged FZDs being recognized by the FZD7 antibody. B: Flow cytometry analysis of the tagged FZDs and FZD7 being expressed on the cell surface. Grey histograms represent untransfected HEK 293T3KO cells. C: Activation of the stable lines of FZD receptors; FZD7, FZD2, FZD9, FZD2-8AA, FZD9-8AA with Wnt3a conditioned media, Wnt mimetic conditioned media and untreated conditioned media for 24 hours.

5

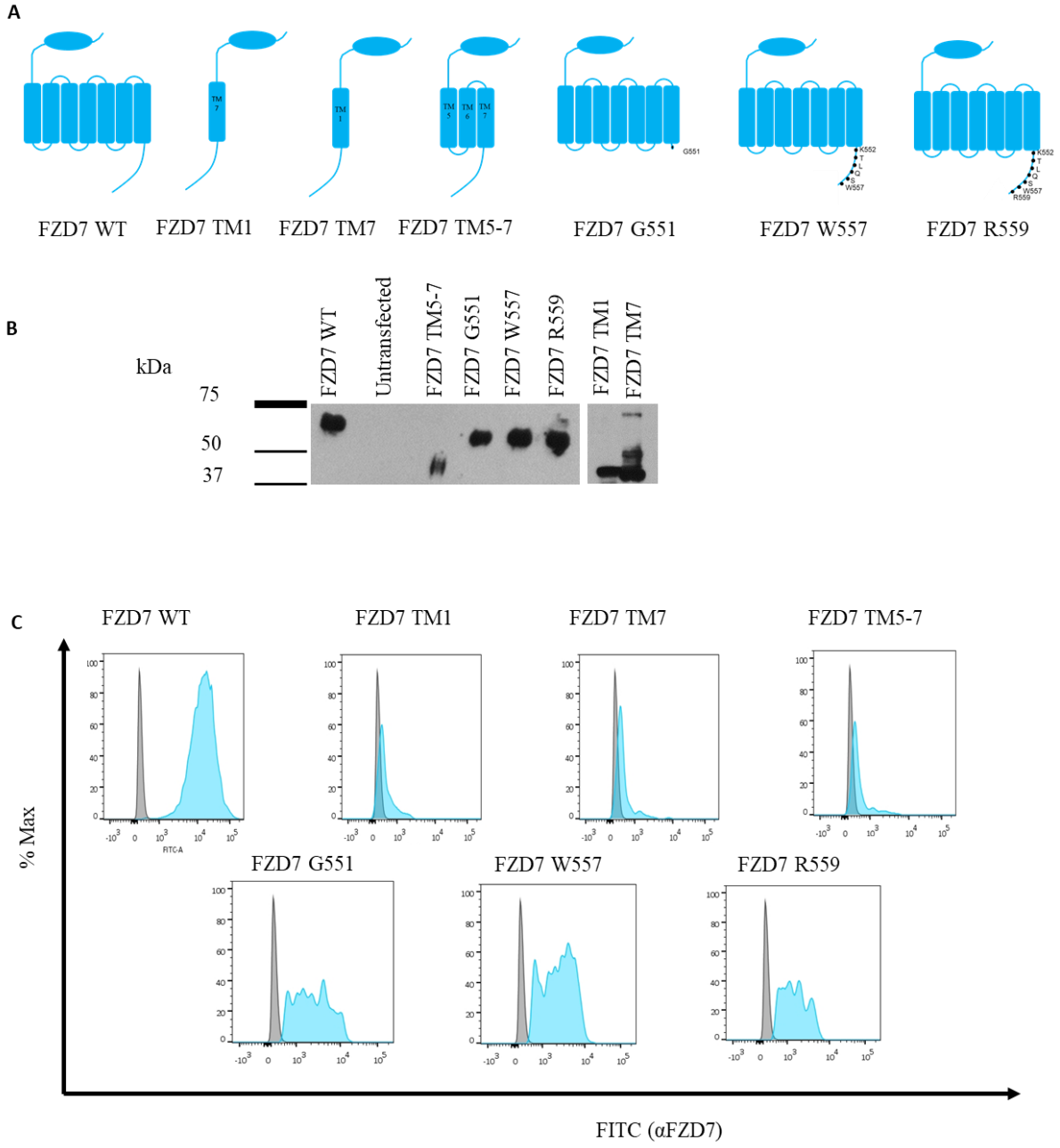

Figure 5: Generation and expression of FZD7 transmembrane domain deletions and tail truncations. A. Schematic of FZD7 constructs generated. B: Western blot probed for FZD7, where the constructs were expressed in HEK293T FZD 1, 2, and 7 KO cells. C: Flow cytometry of FZD7 constructs with an IRES mKate fluorophore against a FZD7 antibody conjugated to FITC. Grey histograms represent untransfected HEK 293T3KO cells, and blue histograms represent the transfected construct.

6

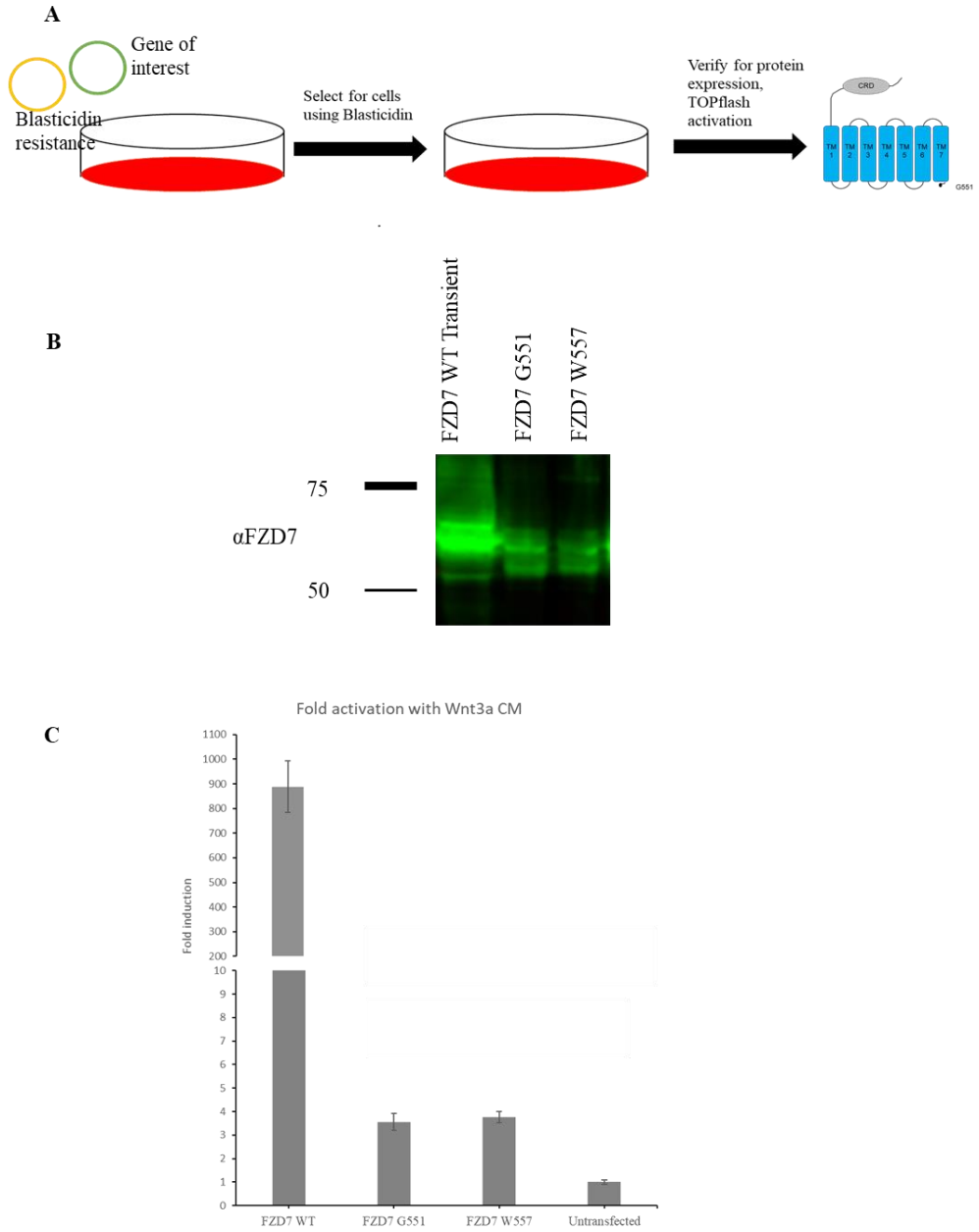

Figure 6: Expression and testing of stable cell lines containing FZD7 with tail truncations. A: Schematic of how the stable lines were generated and tested. B: Western blot of the stable line lysates probed with αFZD7 antibody. C: Luciferase assay of FZD7 WT, FZD7 G551 and FZD7 W557 using Wnt3a condition media, treated for 24 h. Y-axis: average light units normalized to HEK293tTF 3KO cell line.

7

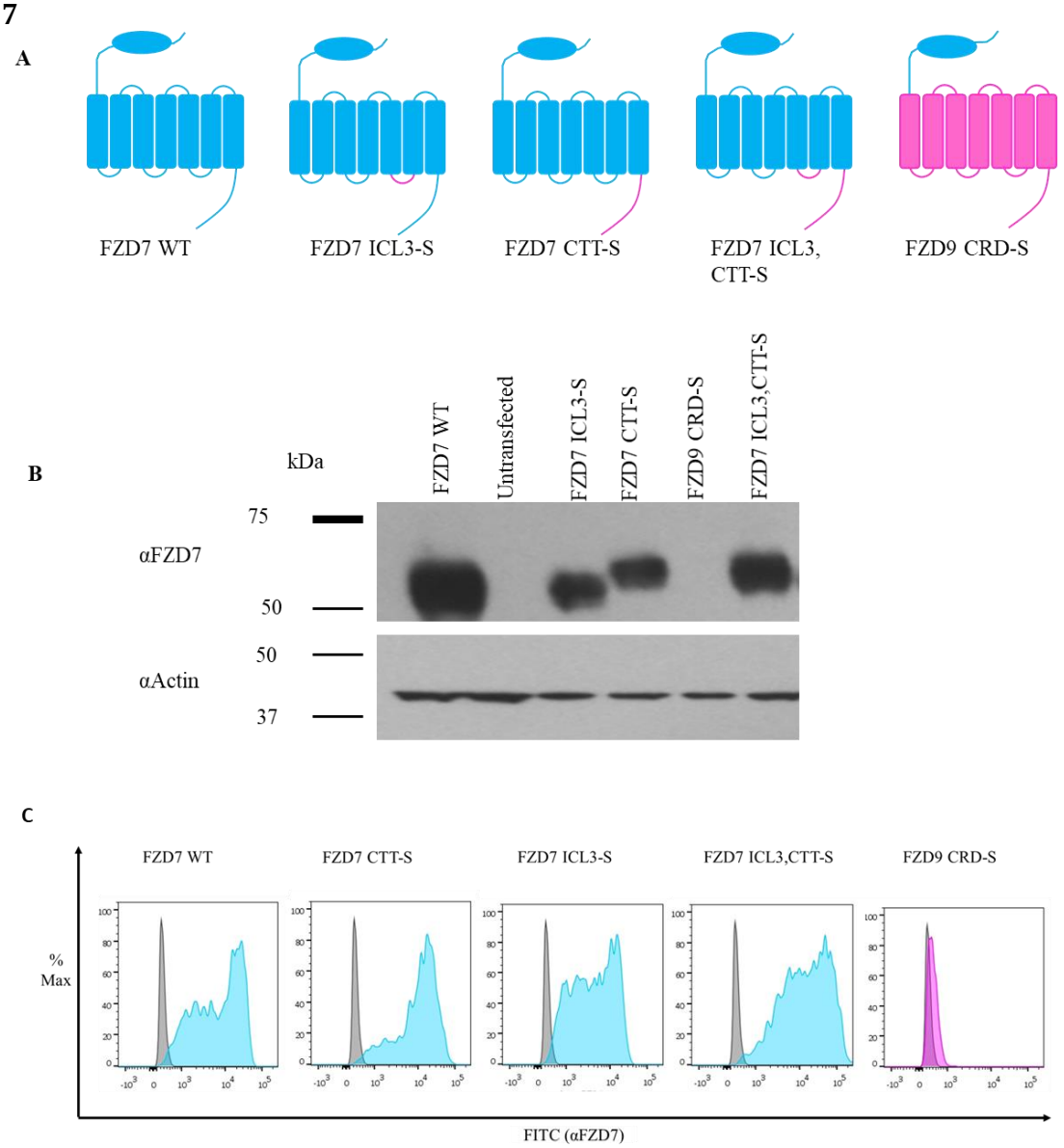

Figure 7: Generation and expression of FZD7 swaps with FZD9. A: Schematic of FZD7 constructs generated, where –S indicates that it has been swapped. FZD7 is denoted in blue and FZD9 in pink. B: Western blot probed for FZD7, where the constructs were expressed in HEK293T FZD 1, 2, and 7 KO cells. C: Flow cytometry of FZD7 constructs with an IRES mKate fluorophore against a FZD7 antibody conjugated to FITC.Grey histograms represent untransfected HEK 293T3KO cells, and blue histograms represent the transfected construct.

8

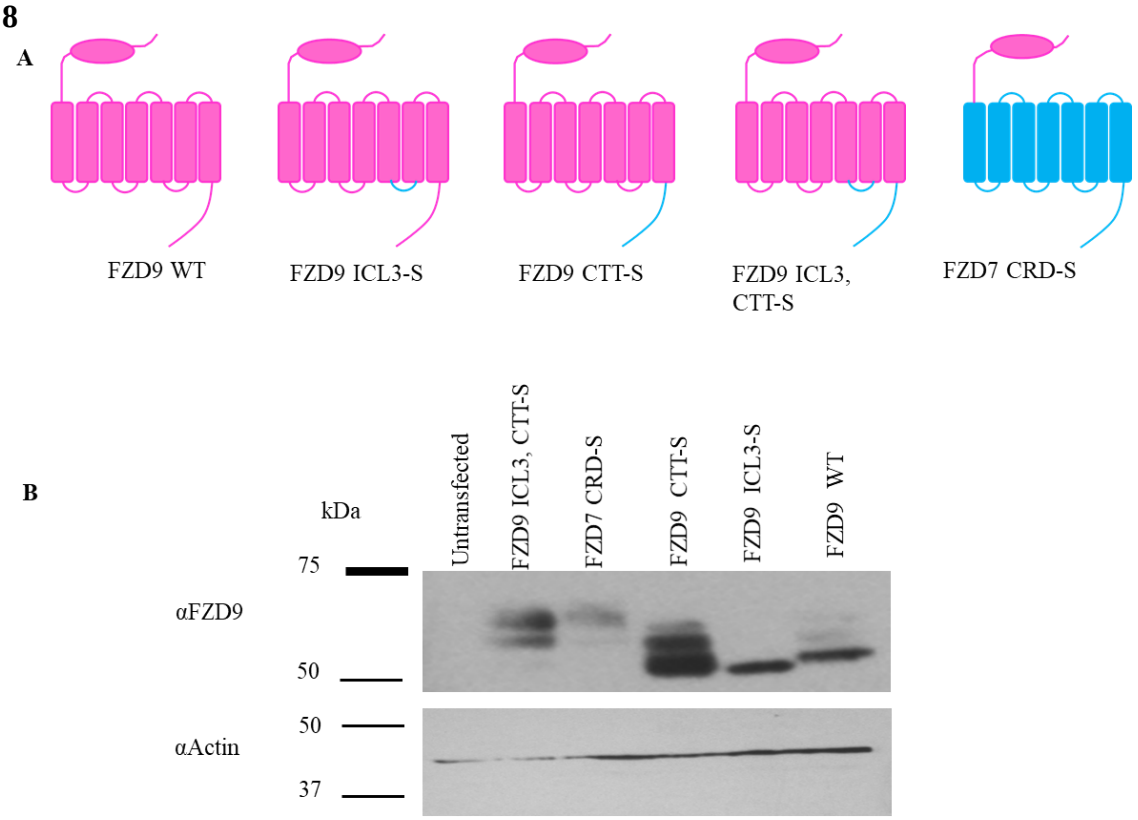

Figure 8: Generation and expression of FZD9 swaps with FZD7. A: Schematic of FZD9 constructs generated, where –S indicates that it has been swapped. FZD7 is denoted in blue and FZD9 is in pink**.** B: Western blot probed for FZD9, where the constructs were expressed in HEK293T FZD 1, 2, and 7 KO cells.